High risk of patient self-inflicted lung injury in COVID-19 with frequently encountered spontaneous breathing patterns: a computational modelling study

Authors: Liam Weaver[1#], Anup Das[1#], Sina Saffaran[2], Nadir Yehya[3], Timothy E. Scott[4], Marc Chikhani[8], John G. Laffey[6], Jonathan G. Hardman[5,8], Luigi Camporota[7]* and Declan G. Bates[1]*

Affiliations:

1. School of Engineering, University of Warwick, Coventry CV4 7AL, UK.
2. Institute of Healthcare Engineering, University College London, London, WC1E 6BT, UK.
3. Department of Anaesthesiology and Critical Care Medicine, Children's Hospital of Philadelphia, University of Pennsylvania, Philadelphia, PA, USA.
4. Academic Department of Military Anaesthesia and Critical Care, Royal Centre for Defence Medicine, ICT Centre, Birmingham B15 2SQ, UK.
5. Anaesthesia & Critical Care, Division of Clinical Neuroscience, School of Medicine, University of Nottingham, Nottingham NG7 2UH, UK.
6. Anaesthesia and Intensive Care Medicine, School of Medicine, NUI Galway, Ireland.
7. Department of Critical Care, Guy's and St Thomas' NHS Foundation Trust, London, UK.
8. Nottingham University Hospitals NHS Trust, Nottingham NG7 2UH, UK.

#Equal contributions *Co-corresponding authors: luigi.camporota@gstt.nhs.uk (+44-7876-876-952), d.bates@warwick.ac.uk (44-7876-876-952)

Abstract

Background: There is ongoing controversy regarding the potential for increased respiratory effort to generate patient self-inflicted lung injury (P-SILI) in spontaneously breathing patients with COVID-19 acute respiratory failure. However, direct clinical evidence linking increased inspiratory effort to lung injury is scarce. We adapted a recently developed computational simulator that replicates distinctive features of COVID-19 pathophysiology to quantify the mechanical forces that could lead to P-SILI at different levels of respiratory effort. In accordance with recent data, the simulator was calibrated to represent a spontaneously breathing COVID-19 patient with severe hypoxaemia (SaO_2 80.6%) and relatively well-preserved lung mechanics (lung compliance of 47.5 ml/cmH_2O), being treated with supplemental oxygen (FiO_2 = 100%).

Results: Simulations were conducted at tidal volumes (VT) and respiratory rates (RR) of 7 ml/kg and 14 breaths/min (representing normal respiratory effort) and at VT/RR of 15/14, 7/20, 15/20, 10/30, 12/30, 10/35, 12/35, 10/40, 12/40 ml/kg / breaths/min. Lung compliance was unaffected by increased VT but decreased significantly at higher RR. While oxygenation improved, significant increases in multiple indicators of the potential for lung injury were observed at all higher VT/RR combinations tested. Pleural pressure swing increased from 10.1 cmH_2O at baseline to 30 cmH_2O at VT/RR of 15 ml/kg / 20 breaths/min and to 54.6 cmH_2O at 12 ml/kg / 40 breaths/min. Dynamic strain increased from 0.3 to 0.49 at VT/RR of 12 ml/kg / 30 breaths/min, and to 0.6 at 15 ml/kg / 20 breaths/min. Mechanical power increased from 7.83 J/min to 17.7 J/min at VT/RR of 7 ml/kg / 20 breaths/min, and to 240.5 J/min at 12 ml/kg / 40 breaths/min.

Conclusions: Our results suggest that the forces generated during increased inspiratory effort in severe COVID-19 are compatible with the development of P-SILI. If conventional oxygen therapy or non-invasive ventilation is ineffective in reducing respiratory effort, control of

driving and transpulmonary pressures with invasive ventilation may reduce the risk of P-SILI and allow time for the resolution of the underlying condition.

Keywords: COVID-19, acute respiratory failure, hypoxaemia, patient self-inflicted lung injury

Introduction

On admission, some patients with COVID-19 acute hypoxaemic respiratory failure (AHRF) exhibit profound hypoxaemia, combined with relatively preserved lung compliance and lung gas volume on CT chest imaging, and substantial increases in respiratory effort - tidal volumes (VT) up to 20 ml/kg (1) and respiratory rates (RR) exceeding 24 breaths/min (2) have been reported. There is currently significant debate regarding whether such increased respiratory effort could risk causing further damage to the lungs through patient self-inflicted lung injury (P-SILI) (3-11).

Direct evidence for the existence of P-SILI in the context of purely spontaneous breathing is largely based on animal studies (12), although two studies in asthmatic children suggested that increased breathing effort could promote negative pressure pulmonary oedema (13, 14). A number of studies have also established the potential for injurious effects due to spontaneous breathing during mechanical ventilation in acute respiratory failure (15). In the context of COVID-19, a recent study has asserted an association between increased respiratory effort and worsening of respiratory function during attempts to wean patients from mechanical ventilation, although without definitively establishing a delineation between cause and effect (9-11, 16). Two recent case reports also noted the existence of spontaneous

pneumothorax and pneumomediastinum in COVID-19 patients, suggesting the generation of injurious transpulmonary pressures (17, 18).

To obtain some additional evidence with which to inform debate on this issue, we hypothesised that a computational model of COVID-19 pathophysiology could be used to investigate the effects of increased respiratory effort on parameters that have been associated with lung injury, namely tidal swings in pleural and transpulmonary pressure, and maximum values of mechanical power (19) and dynamic strain.

Methods

The core model used in this study is a multi-compartmental computational simulator that has been previously used to simulate mechanically ventilated patients with various pulmonary disease states (20-27), including COVID-19 ARDS (28). The simulator offers several advantages, including the capability to define a large number of alveolar compartments (each with its own individual mechanical characteristics), with configurable alveolar collapse, alveolar stiffening, disruption of alveolar gas-exchange, pulmonary vasoconstriction and vasodilation, and airway obstruction. As a result, several defining, clinical features of acute lung injury can be represented in the model, including varying degrees of ventilation perfusion mismatch, physiological shunt and deadspace, alveolar gas trapping with intrinsic positive end-expiratory pressure (PEEP), collapse-reopening of alveoli etc. A detailed description of the physiological principles and mathematical equations underlying the computational model implemented in the simulator is provided in the supplementary file.

For the current study, the model was configured to represent a patient of 70 kg ideal body weight with COVID-19 acute respiratory failure. Based on currently available data regarding potential pathophysiological mechanisms e.g. (29-34), the model provides a heterogeneous disease profile distributed across 100 gas-exchanging compartments implementing (a)

vasodilation leading to hyperperfusion of collapsed lung regions, (b) disruption of hypoxic pulmonary vasoconstriction, with hypoperfusion of normally aerated lung regions (c) disruption of alveolar gas-exchange due to the effects of pneumonitis, and (d) heightened vascular resistance due to the presence of microthrombi, while maintaining relatively well preserved lung compliance and gas volumes. It replicates closely the levels of ventilation-perfusion mismatch and hypoxemia (34, 35), as well as the lack of responsiveness to PEEP (36-38), that has been documented in some patients with COVID-19; see (28) and the supplementary file for full details.

For the investigation of P-SILI, the model was adapted to represent spontaneously breathing patients. Spontaneous breathing is simulated by incorporating the variable P_{MUS}, which represents the pressure generated by the respiratory muscles acting on the lung. P_{MUS} is modelled as a piecewise function as described in (39) and adapted from (40). The function consists of a parabolic profile during the inspiration phase of the respiratory cycle, representing the progressive increase in pressure exerted by the respiratory muscles, followed by an exponential profile during the expiration phase of the respiratory cycle, characterizing the passive relaxation of the muscles. Accordingly,

$$P_{MUS}(t) = \begin{cases} \frac{-P_{MIN}}{T_I.T_E}.t^2 + \frac{P_{MIN}.T}{T_I.T_E}.t & t \in \lfloor 0, T_I \rfloor \\ \frac{P_{MIN}}{1 - e^{-\frac{T_E}{\tau}}}.\left(e^{-\frac{(t-T_I)}{\tau}} - e^{-\frac{T_E}{\tau}}\right) & t \in \lfloor T_I, T \rfloor \end{cases}$$

P_{MUS} decreases from zero to its minimum end-inspiratory value (P_{MIN}) (i.e., maximum effort). T is calculated from the set respiratory rate, RR, (T = 60/RR). T_I and T_E are the duration of inspiration and expiration, such that ($T = T_I + T_E$). T_I is calculated from ($T_I = T * DC$) where DC is the duty cycle, set to 0.33. τ is the time constant of the expiratory profile and is set to 5 seconds.

The resultant alveolar pressure P_{ALV} depends on P_{MUS}, as well as on the pressures of the gases within the compartment, the stiffness of the compartment (S_N), and parameter $P_{EXT,N}$ which represents extrinsic pressures acting on the compartment. Pleural pressure is calculated as

$$P_{Pl} = P_{ALV} - \frac{V_L - V_{u,L}}{C_{CW}}$$

where V_L is the total lung volume, C_{CW} is the compliance of the chest wall, which is set to 0.2 L/cmH_2O (40), and $V_{u,L}$ is the unstressed volume of the lung (set to 1L).

To observe the pulmonary effects of interest, the following values were computed and recorded: arterial oxygen partial pressure (PaO_2), arterial carbon dioxide partial pressure ($PaCO_2$), arterial pH (pH), arterial oxygen saturation of haemoglobin (SaO_2), volume and pressure of individual alveolar compartments at end-inspiration and end-expiration (V_{ALV_insp}, V_{ALV_exp} and P_{ALV_insp} and V_{ALV_exp}, respectively), cardiac output (CO), pleural pressure, and transpulmonary pressure (P_{TP}), calculated as the difference between the lung pressure and pleural pressure. Shunt fraction (Q_S/Q_T) was calculated using the classical shunt equation, based on the calculated values of arterial, pulmonary end-capillary and mixed venous O_2 content. Physiological deadspace (and deadspace fraction; VD/VT) were calculated from $PaCO_2$, mixed expired CO_2 pressure ($P\bar{E}CO_2$) and the exhaled tidal volume.

A range of indices associated with the risk of P-SILI were recorded, including the transpulmonary and pleural pressure swings, dynamic strain (calculated as VT / end expiratory lung volume), and the mechanical power applied to the lungs, calculated as:

$$Power = 0.098 \times \mathrm{RR} \times \left\{ VT^2 \times \left[0.5 \times EL_{rs} + \mathrm{RR} \times \frac{(1 + I{:}E)}{60 \times I{:}E} \times R_{aw} \right] \right\} \qquad (1)$$

where EL_{rs} is the lung elastance (calculated as variation in total lung pressure during a breath (ΔP_L) divided by the tidal volume), $I{:}E$ is the inspiratory-to-expiratory time ratio, and R_{aw} is

the airway resistance (calculated as the driving pressure generated by P_{MUS} divided by the average flow rate during inspiration).

All model simulations were run for 30 minutes, with the reported data averaged over the final 1 minute, and conducted using Matlab version R2019b.v9 (MathWorks Inc., Natick, MA, USA).

Results

The simulated patient replicates levels of hypoxaemia that have frequently been reported in spontaneously breathing COVID-19 patients. SaO_2, PaO_2 and $PaCO_2$ on 100% oxygen at baseline were 80.6%, 48.06 mmHg, and 58.43 mmHg, respectively (Table 1). Oxygenation improved at higher respiratory efforts (SaO_2 of 99.7% at VT / RR of 12 ml/kg / 40 breath/min) and $PaCO_2$ decreased. Values of lung compliance and functional residual capacity (FRC) at baseline were 47.5 ml/cmH_2O and 1743.6 ml, showing good agreement with the data for a cohort of COVID-19 patients reported in a recent study (average values for lung compliance and lung gas volume of 49.9 ml/cmH_2O and 1670 ml, respectively, (41)). Lung compliance was unaffected by increased VT but reduced significantly at higher respiratory rates (to 32.9 ml/cmH2O at VT / RR of 7 ml/kg / 20 breath/min, and 15.6 ml/cmH2O at 10 ml/kg / 40 breaths/min). Physiological shunt / deadspace were decreased / increased at higher respiratory effort (minimum shunt of 25.8% at VT / RR of 12 ml/kg / 40 breath/min, maximum deadspace of 369.7 ml at VT / RR of 15 ml/kg / 20 breath/min).

Muscle pressures required to generate the different increased breathing patterns (maximum P_{MUS} of 64.9 cmH_2O at VT / RR of 12 ml/kg / 40 breath/min) were well within the limits specified for a 70kg adult male (maximum P_{MUS} of 78.5 cmH_2O at age 60, and 108.9 cmH_2O at age 40, (42)).

As shown in Fig. 1 and Table 1, significant increases in multiple indicators of the potential for lung injury were observed at all higher VT / RR combinations tested. Pleural pressure swing increased from 10.2 cmH_2O at baseline to 30 cmH_2O at VT / RR of 15 ml/kg / 20 breaths/min, up to a maximum of 52.9 cmH_2O at 12 ml/kg / 40 breaths/min. Dynamic strain increased from 0.3 to 0.49 at VT / RR of 12 ml/kg / 30 breaths/min, up to a maximum of 0.6 at 15 ml/kg / 20 breaths/min. Mechanical power increased from 7.83 J/min to 17.7 J/min at VT / RR of 7 ml/kg / 20 breaths/min, and up to a maximum of 239.9 J/min at 12 ml/kg / 40 breaths/min.

The effect of increased respiratory effort on the distribution of maximum alveolar compartmental volumes is shown in Fig. 2 here and Fig.1.3 in supplementary file. The model consists of 100 independently configured gas-exchanging compartments. Compartments 93 to 100 are collapsed at baseline, at greater respiratory effort some of these compartments are partially recruited. As shown, at the higher values of tidal volume and respiratory rate, the proportion of compartments experiencing larger maximum volumes is significantly increased.

Discussion

During mechanical ventilation, the power required to inflate the lungs is provided by an external source of energy, whereas during spontaneous unassisted breathing it is provided by the respiratory muscles. However, as pointed out in (19), lung injury (in the sense of mechanical lesions in the interstitial space due to microfractures of the extracellular matrix or the capillary walls) arises from the mechanical energy applied to the lungs, which generates the relevant pressures. There is therefore no reason to believe that the extent of injury will be significantly different whether excessive pressures are generated by respiratory muscles in spontaneous breathing or by a mechanical ventilator. Similarly to the case of VILI, there is

also no reason to expect that, in the case of injured lungs, forces generated by respiratory muscles could not lead to injurious effects on a regional level due to lung heterogeneity.

While the levels of transpulmonary pressure at higher respiratory effort in our model were well within generally accepted safe limits, we observed large increases in pleural pressure swings, up to a maximum of 30 cmH_2O. Interestingly, in a recent study of inspiratory effort in non-invasive ventilation, reductions in pleural pressure (recorded as oesophageal pressure using a multifunctional nasogastric tube with a dedicated pressure transducer) of 10 cm H_2O or more after 2 hours of treatment was strongly associated with avoidance of intubation and represented the most accurate predictor of treatment success (43). Also, as discussed in (44), negative alveolar pressures created by large changes in pleural pressure, and therefore positive changes in transvascular pressure, favour lung edema, a mechanism that is amplified with increased vascular permeability, (45, 46). Given that negative pressures from diaphragm contraction are not distributed uniformly, there is also the potential to cause pendelluft gas movement due to localised changes in pleural pressures in dependent regions, (47). Finally, it is important to recognise that when dynamic systems (from aircraft engines to human lungs) are subjected to repeated cycles of excessive stresses and strains, their deterioration over time is often not linear; rather, damage can accumulate "silently" before eventually manifesting and spreading rapidly (48).

In light of the above considerations, it is difficult to see how, for a respiratory effort that a patient (and their treating clinician) might consider tolerable, the levels of pleural pressure swing, mechanical power, and dynamic strain produced in our model (Table 1), as well as the corresponding skewing of compartmental volumes towards higher values (Fig. 2), could be regarded as safe. Certainly, it is unlikely that any mechanical ventilation strategy that produced similar values would be considered "protective" according to current standard guidelines. Our results also highlight that improvements in PaO_2/FiO_2 ratio associated with

larger tidal volume and respiratory rate should be interpreted in the context of the associated increased respiratory effort and are not necessarily expressions of improved lung condition. Indeed, the improvement in PaO_2/FiO_2 ratio we observed at higher respiratory effort was coupled with reduced lung compliance and the development of levels of mechanical power associated with worse short (49, 50) and long term (51) survival.

The debate around the potential role of P-SILI in contributing to the rapid deterioration observed in some COVID-19 patients is a vigorous one, but we would suggest that it is unnecessary to adopt extreme positions regarding the resulting implications for timing of intubation. While more evidence is gathered, it is surely prudent is to adopt a "protective ventilation" strategy, i.e. carefully monitor, and seek to reduce, high respiratory effort in such patients, via either standard supplemental oxygen treatment or non-invasive ventilation. If these options fail to promptly reduce high respiratory effort even after resolution of hypoxaemia, then controlling driving and transpulmonary pressure through mechanical ventilation and the institution of strategies such as prone positioning should be initiated in a timely fashion to avoid the potential additional risks associated with P-SILI.

On this point, a recent case-study described in (8) may illustrate those risks. The author reports a patient who presented to the emergency department with moderate respiratory distress and increased respiratory effort. After initial treatment with supplemental oxygen via a non-rebreather facemask followed by a failed trial of bilevel positive airway pressure, she required tracheal intubation 5 hours later. The chest X-ray (CXR) at the time of intubation "showed a remarkable progression of infiltrates since the admission CXR". The author notes that "while worsening pneumonia could have contributed to her CXR findings, it is hard to overlook the contribution of P-SILI to her worsening pulmonary infiltrates".

Our study has some limitations, principally that the results are based on computational modeling of COVID-19 pathophysiology, rather than data from patients with COVID-19.

Investigating the issues raised here in clinical trials is likely to prove challenging both from an ethical and practical point of view, however, and suitable animal models of COVID-19 pathophysiology to study these questions are yet to emerge (52). In these circumstances, we hope that insights from detailed computational models that recapitulate patient breathing patterns and lung mechanics can provide useful evidence with which to inform current debate.

Conclusions

Our results indicate that pressures compatible with the occurrence of P-SILI can develop in patients with COVID-19 acute respiratory failure who experience only moderately increased respiratory effort, i.e. without overt dyspnoea, through significant increases in pleural pressure swings, mechanical power and dynamic strain. If conventional oxygen therapy or non-invasive ventilation is ineffective in reducing respiratory effort, control of driving and transpulmonary pressures with invasive ventilation may reduce the effects of P-SILI and allow time for the resolution of the underlying condition.

References

1. Gattinoni L, Chiumello D, Caironi P, Busana M, Romitti F, Brazzi L, et al. COVID-19 pneumonia: different respiratory treatments for different phenotypes? Intensive Care Med. 2020;46(6):1099-102.
2. Nicholson TW, Talbot NP, Nickol A, Chadwick AJ, Lawton O. Respiratory failure and non-invasive respiratory support during the covid-19 pandemic: an update for re-deployed hospital doctors and primary care physicians. BMJ. 2020;369:m2446.
3. Gattinoni L, Marini JJ, Busana M, Chiumello D, Camporota L. Spontaneous breathing, transpulmonary pressure and mathematical trickery. Ann Intensive Care. 2020;10(1):88.
4. Tobin MJ, Laghi F, Jubran A. P-SILI is not justification for intubation of COVID-19 patients. Ann Intensive Care. 2020;10(1):105.
5. Tobin MJ, Jubran A, Laghi F. P-SILI as justification for intubation in COVID-19: readers as arbiters. Ann Intensive Care. 2020;10(1):156.

6. Gattinoni L, Marini JJ, Chiumello D, Busana M, Camporota L. COVID-19: scientific reasoning, pragmatism and emotional bias. Ann Intensive Care. 2020;10(1):134.

7. Cruces P, Retamal J, Hurtado DE, Erranz B, Iturrieta P, Gonzalez C, et al. A physiological approach to understand the role of respiratory effort in the progression of lung injury in SARS-CoV-2 infection. Crit Care. 2020;24(1):494.

8. Matta S. Dilemmas in Covid-19 respiratory distress: Early vs late intubation; high tidal volume and low PEEP vs traditional approach. J Intensive Critical Care. 2020;6:7.

9. Gattinoni L, Marini JJ, Camporota L. The Respiratory Drive: An Overlooked Tile of COVID-19 Pathophysiology. Am J Respir Crit Care Med. 2020;202(8):1079-80.

10. Tobin MJ, Jubran A, Laghi F. Respiratory Drive Measurements Do Not Signify Conjectural Patient Self-inflicted Lung Injury. Am J Respir Crit Care Med. 2021;203(1):142-3.

11. Gattinoni L, Marini JJ, Camporota L. Reply to Tobin et al.: Respiratory Drive Measurements Do Not Signify Conjectural Patient Self-inflicted Lung Injury. Am J Respir Crit Care Med. 2021;203(1):143-4.

12. Mascheroni D, Kolobow T, Fumagalli R, Moretti MP, Chen V, Buckhold D. Acute respiratory failure following pharmacologically induced hyperventilation: an experimental animal study. Intensive Care Med. 1988;15(1):8-14.

13. Dunnill MS. The pathology of asthma, with special reference to changes in the bronchial mucosa. J Clin Pathol. 1960;13:27-33.

14. Stalcup SA, Mellins RB. Mechanical forces producing pulmonary edema in acute asthma. N Engl J Med. 1977;297(11):592-6.

15. Brochard L. Ventilation-induced lung injury exists in spontaneously breathing patients with acute respiratory failure: Yes. Intensive Care Med. 2017;43(2):250-2.

16. Esnault P, Cardinale M, Hraiech S, Goutorbe P, Baumstrack K, Prud'homme E, et al. High Respiratory Drive and Excessive Respiratory Efforts Predict Relapse of Respiratory Failure in Critically Ill Patients with COVID-19. Am J Respir Crit Care Med. 2020;202(8):1173-8.

17. Alharthy A, Bakirova GH, Bakheet H, Balhamar A, Brindley PG, Alqahtani SA, et al. COVID-19 with spontaneous pneumothorax, pneumomediastinum, and subcutaneous emphysema in the intensive care unit: Two case reports. J Infect Public Health. 2020;14(3):290-2.

18. Rafiee MJ, Babaki Fard F, Samimi K, Rasti H, Pressacco J. Spontaneous pneumothorax and pneumomediastinum as a rare complication of COVID-19 pneumonia: Report of 6 cases. Radiol Case Rep. 2021;16(3):687-92.

19. Gattinoni L. Ventilation-induced lung injury exists in spontaneously breathing patients with acute respiratory failure: We are not sure. Intensive Care Med. 2017;43(2):256-8.

20. McCahon R, Columb M, Mahajan R, Hardman J. Validation and application of a high-fidelity, computational model of acute respiratory distress syndrome to the examination of the indices of oxygenation at constant lung-state. British journal of anaesthesia. 2008;101(3):358-65.

21. Das A, Cole O, Chikhani M, Wang W, Ali T, Haque M, et al. Evaluation of lung recruitment maneuvers in acute respiratory distress syndrome using computer simulation. Critical Care. 2015;19(1):8.

22. Chikhani M, Das A, Haque M, Wang W, Bates DG, Hardman JG. High PEEP in acute respiratory distress syndrome: quantitative evaluation between improved arterial oxygenation and decreased oxygen delivery. Br J Anaesth. 2016;117(5):650-8.

23. Das A, Haque M, Chikhani M, Cole O, Wang W, Hardman JG, et al. Hemodynamic effects of lung recruitment maneuvers in acute respiratory distress syndrome. BMC Pulm Med. 2017;17(1):34.

24. Das A, Camporota L, Hardman JG, Bates DG. What links ventilator driving pressure with survival in the acute respiratory distress syndrome? A computational study. Respir Res. 2019;20(1):29.

25. Saffaran S, Das A, Hardman JG, Yehya N, Bates DG. High-fidelity computational simulation to refine strategies for lung-protective ventilation in paediatric acute respiratory distress syndrome. Intensive Care Med. 2019;45(7):1055-7.

26. Saffaran S, Das A, Laffey JG, Hardman JG, Yehya N, Bates DG. Utility of Driving Pressure and Mechanical Power to Guide Protective Ventilator Settings in Two Cohorts of Adult and Pediatric Patients With Acute Respiratory Distress Syndrome: A Computational Investigation. Crit Care Med. 2020;48(7):1001-8.

27. Scott TE, Haque M, Das A, Cliff I, Bates DG, Hardman JG. Efficacy of continuous positive airway pressure in casualties suffering from primary blast lung injury: A modeling study. Annu Int Conf IEEE Eng Med Biol Soc. 2019;2019:4965-8.

28. Das A, Saffaran S, Chikhani M, Scott TE, Laviola M, Yehya N, et al. In Silico Modeling of Coronavirus Disease 2019 Acute Respiratory Distress Syndrome: Pathophysiologic Insights and Potential Management Implications. Crit Care Explor. 2020;2(9):e0202.

29. Lang M, Som A, Mendoza DP, Flores EJ, Reid N, Carey D, et al. Hypoxaemia related to COVID-19: vascular and perfusion abnormalities on dual-energy CT. Lancet Infect Dis. 2020;20(12):1365-6.

30. Albarello F, Pianura E, Di Stefano F, Cristofaro M, Petrone A, Marchioni L, et al. 2019-novel Coronavirus severe adult respiratory distress syndrome in two cases in Italy: An uncommon radiological presentation. Int J Infect Dis. 2020;93:192-7.

31. Helms J, Tacquard C, Severac F, Leonard-Lorant I, Ohana M, Delabranche X, et al. High risk of thrombosis in patients with severe SARS-CoV-2 infection: a multicenter prospective cohort study. Intensive Care Med. 2020;46(6):1089-98.

32. Menter T, Haslbauer JD, Nienhold R, Savic S, Hopfer H, Deigendesch N, et al. Postmortem examination of COVID-19 patients reveals diffuse alveolar damage with severe capillary congestion and variegated findings in lungs and other organs suggesting vascular dysfunction. Histopathology. 2020;77(2):198-209.

33. Jain A, Doyle DJ. Stages or phenotypes? A critical look at COVID-19 pathophysiology. Intensive Care Med. 2020;46(7):1494-5.

34. Gattinoni L, Coppola S, Cressoni M, Busana M, Rossi S, Chiumello D. COVID-19 Does Not Lead to a "Typical" Acute Respiratory Distress Syndrome. Am J Respir Crit Care Med. 2020;201(10):1299-300.

35. Marini JJ, Gattinoni L. Management of COVID-19 Respiratory Distress. JAMA. 2020;323(22):2329-30.

36. Roesthuis L, van den Berg M, van der Hoeven H. Advanced respiratory monitoring in COVID-19 patients: use less PEEP! Crit Care. 2020;24(1):230.

37. Tsolaki V, Siempos I, Magira E, Kokkoris S, Zakynthinos GE, Zakynthinos S. PEEP levels in COVID-19 pneumonia. Crit Care. 2020;24(1):303.

38. Bonny V, Janiak V, Spadaro S, Pinna A, Demoule A, Dres M. Effect of PEEP decremental on respiratory mechanics, gasses exchanges, pulmonary regional ventilation, and hemodynamics in patients with SARS-Cov-2-associated acute respiratory distress syndrome. Crit Care. 2020;24(1):596.

39. Mecklenburgh JS, Mapleson WW. Ventilatory assistance and respiratory muscle activity. 2: Simulation with an adaptive active ("aa" or "a-squared") model lung. Br J Anaesth. 1998;80(4):434-9.

40. Albanese A, Cheng L, Ursino M, Chbat NW. An integrated mathematical model of the human cardiopulmonary system: model development. Am J Physiol Heart Circ Physiol. 2016;310(7):H899-921.

41. Chiumello D, Busana M, Coppola S, Romitti F, Formenti P, Bonifazi M, et al. Physiological and quantitative CT-scan characterization of COVID-19 and typical ARDS: a matched cohort study. Intensive Care Med. 2020;46(12):2187-96.

42. Harik-Khan RI, Wise RA, Fozard JL. Determinants of maximal inspiratory pressure. The Baltimore Longitudinal Study of Aging. Am J Respir Crit Care Med. 1998;158(5 Pt 1):1459-64.

43. Tonelli R, Fantini R, Tabbi L, Castaniere I, Pisani L, Pellegrino MR, et al. Early Inspiratory Effort Assessment by Esophageal Manometry Predicts Noninvasive Ventilation Outcome in De Novo Respiratory Failure. A Pilot Study. Am J Respir Crit Care Med. 2020;202(4):558-67.

44. Brochard L, Slutsky A, Pesenti A. Mechanical Ventilation to Minimize Progression of Lung Injury in Acute Respiratory Failure. Am J Respir Crit Care Med. 2017;195(4):438-42.

45. Grieco DL, Menga LS, Eleuteri D, Antonelli M. Patient self-inflicted lung injury: implications for acute hypoxemic respiratory failure and ARDS patients on non-invasive support. Minerva Anestesiol. 2019;85(9):1014-23.

46. Arnal JM, Chatburn R. Paying attention to patient self-inflicted lung injury. Minerva Anestesiol. 2019;85(9):940-2.

47. Yoshida T, Roldan R, Beraldo MA, Torsani V, Gomes S, De Santis RR, et al. Spontaneous Effort During Mechanical Ventilation: Maximal Injury With Less Positive End-Expiratory Pressure. Crit Care Med. 2016;44(8):e678-88.

48. Bhat S, Patibandla R. Metal fatigue and basic theoretical models: a review. Alloy Steel-Properties and Use. 2011;22.

49. Neto AS, Deliberato RO, Johnson AE, Bos LD, Amorim P, Pereira SM, et al. Mechanical power of ventilation is associated with mortality in critically ill patients: an analysis of patients in two observational cohorts. Intensive care medicine. 2018;44(11):1914-22.

50. Zhang Z, Zheng B, Liu N, Ge H, Hong Y. Mechanical power normalized to predicted body weight as a predictor of mortality in patients with acute respiratory distress syndrome. Intensive Care Med. 2019;45(6):856-64.

51. Parhar KKS, Zjadewicz K, Soo A, Sutton A, Zjadewicz M, Doig L, et al. Epidemiology, Mechanical Power, and 3-Year Outcomes in Acute Respiratory Distress Syndrome Patients Using Standardized Screening. An Observational Cohort Study. Ann Am Thorac Soc. 2019;16(10):1263-72.

52. Ehaideb SN, Abdullah ML, Abuyassin B, Bouchama A. Evidence of a wide gap between COVID-19 in humans and animal models: a systematic review. Critical Care. 2020;24(1):1-23.

Supplementary Materials

1) P-SILI_Supplementary.pdf – Full description of computational simulator and additional figures.

Funding: UK Engineering and Physical Sciences Research Council (grants EP/P023444/1 and EP/V014455/1).

Competing interests: The authors declare that they have no competing interests.

Materials and Correspondence: Requests to be forwarded to Prof. Declan G Bates.

	VT = 7 (ml/kg), RR = 14 (b/min)	VT = 15 (ml/kg), RR = 14 (b/min)	VT = 7 (ml/kg), RR = 20 (b/min)	VT = 15 (ml/kg), RR = 20 (b/min)	VT = 10 (ml/kg), RR = 30 (b/min)	VT = 12 (ml/kg), RR = 30 (b/min)	VT = 10 (ml/kg), RR = 35 (b/min)	VT = 12 (ml/kg), RR = 35 (b/min)	VT = 10 (ml/kg), RR = 40 (b/min)	VT = 12 (ml/kg), RR = 40 (b/min)
P_{MUS} (cmH_2O)	-16.5	-37.0	-21.5	-45.0	-42.6	-51.3	-49.0	-57.6	-55.3	-64.9
SaO_2 (%)	80.6	86.4	81.0	93.3	93.2	93.2	93.2	98.5	96.2	99.7
PaO_2 (mmHg)	48.1	49.9	46.7	64.3	63.7	63.2	63.6	107.6	78.0	174.3
PF ratio (mmHg)	48.1	49.9	46.7	64.3	63.7	63.2	63.6	107.6	78.0	174.3
Phys. Shunt (%)	49.3	44.9	49.2	37.7	37.6	37.6	37.6	29.8	33.7	25.8
Phys. VD (ml)	191.7	390.4	192.9	369.7	266.1	320.9	273.9	313.9	272.2	310.5
VD/VT	0.39	0.37	0.39	0.36	0.38	0.38	0.39	0.37	0.39	0.37
$PaCO_2$ (mmHg)	58.4	28.5	41.5	19.6	18.5	15.9	16.2	13.2	14.0	11.5
FRC (ml)	1743.6	1776.2	1790.5	1866.3	1961.9	1999.5	2022.8	2083.3	2101.0	2170.1
VT (ml)	491.0	1045.5	495.8	1034.4	700.3	841.0	700.9	840.5	700.3	839.6
Lung Compliance (ml/cmH_2O)	47.5	47.9	32.9	34.1	21.5	21.8	18.1	18.6	15.6	16.1
DP (cmH_2O)	10.3	21.8	15.1	30.3	32.5	38.6	38.8	45.1	44.8	52.1
Power (J/min)	7.8	34.9	17.7	73.3	88.6	124.8	127.6	176.6	173.7	239.9
Dynamic Strain	0.30	0.62	0.31	0.60	0.42	0.49	0.42	0.48	0.41	0.47
ΔP_{PL}, (cmH_2O)	10.2	21.1	15.2	30.00	32.0	39.2	39.3	45.7	45.6	52.9
ΔP_{TP} (cmH_2O)	2.6	5.5	2.8	5.6	4.1	4.9	4.2	5.0	4.3	5.1

Abbreviations: VT: Tidal Volume, RR: Respiratory Rate, SaO_2: Arterial O_2 Saturation, PaO_2: Arterial O_2 partial pressure, VD: Deadspace, $PaCO_2$: Arterial CO_2 partial pressure, FRC: Functional Residual Capacity, DP: Driving Pressure, P_{PL}: Pleural Pressure, P_{TP}: Transpulmonary pressure

Table 1: Oxygenation, lung mechanics, maximum pressure swings, and other injury indicators generated in our COVID-19 model for different levels of respiratory effort on 100% oxygen.

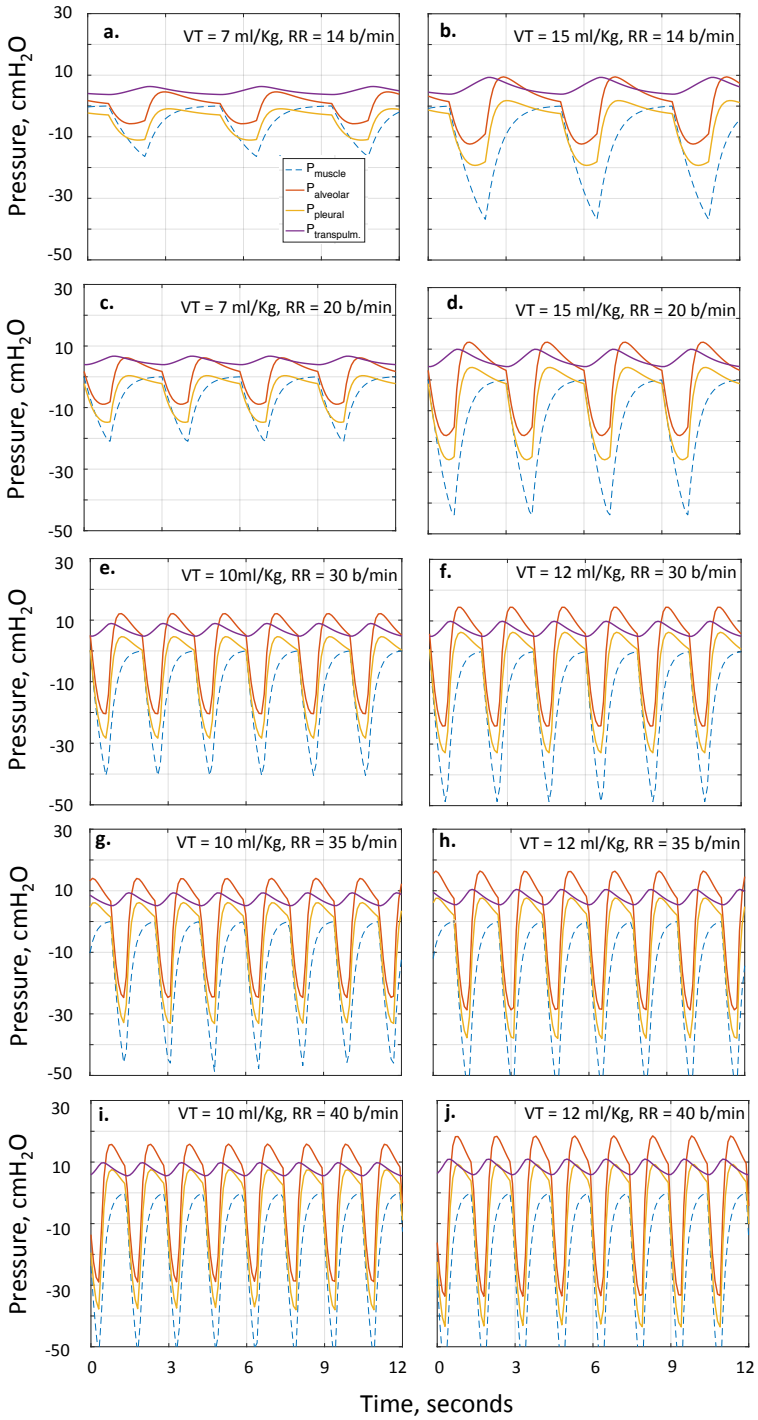

Figure 1: Muscle, pleural, transpulmonary and alveolar pressure swings generated by normal and increased respiratory effort in our COVID-19 model, (a) VT = 7 ml/kg, RR = 14 b/min, (b) VT = 15 ml/kg, RR = 14 b/min, (c) VT = 7 ml/kg, RR = 20 b/min, (d) VT = 15 ml/kg, RR = 20 b/min, (e) VT = 10 ml/kg, RR = 30 b/min, (f) VT = 12 ml/kg, RR = 30 b/min, (g) VT = 10 ml/kg, RR = 35 b/min, (h) VT = 12 ml/kg, RR = 35 b/min, (i) VT = 10 ml/kg, RR = 40 b/min, (j) VT = 12 ml/kg, RR = 40 b/min.

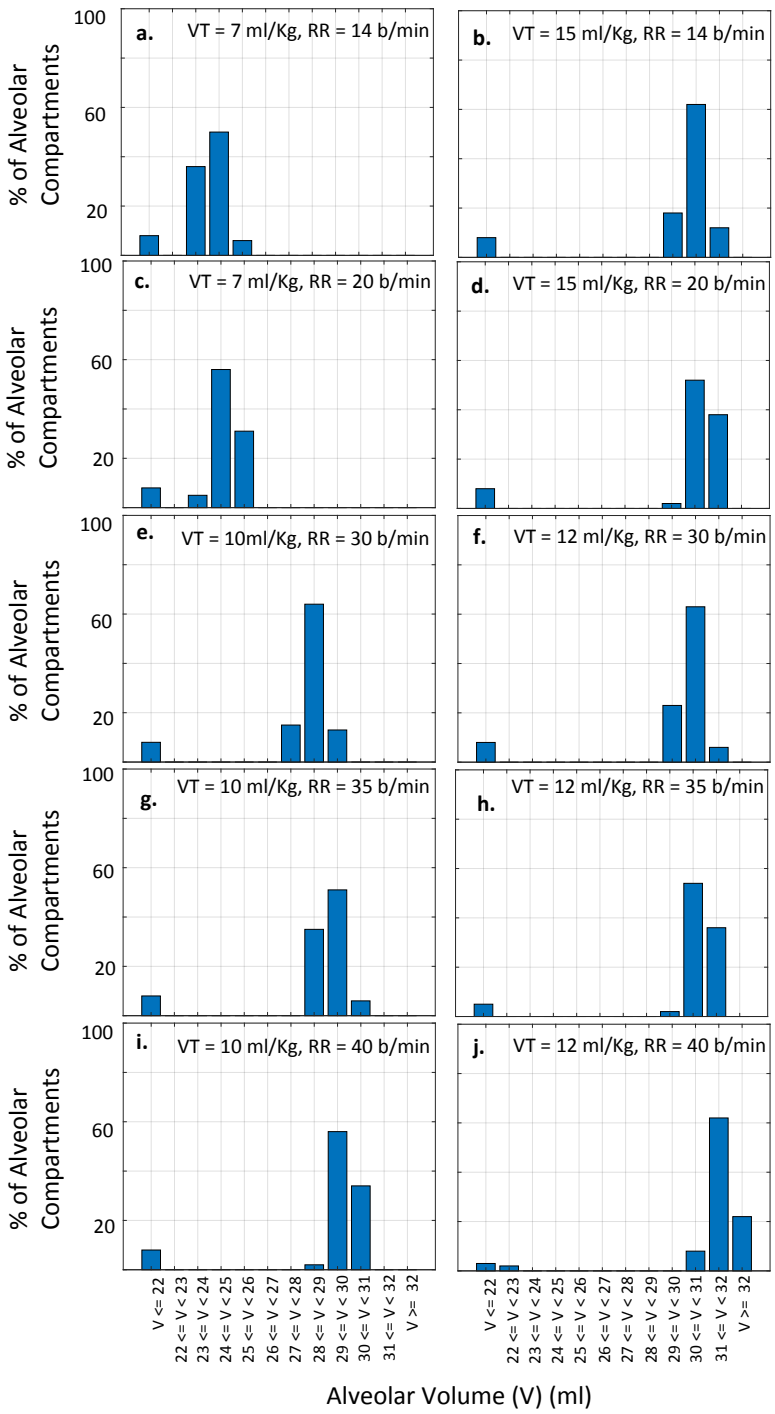

Figure 2: Distribution of maximum compartmental volumes in the model. The model consists of 100 independently configured gas-exchanging compartments. (a) VT = 7 ml/kg, RR = 14 b/min, (b) VT = 15 ml/kg, RR = 14 b/min, (c) VT = 7 ml/kg, RR = 20 b/min, (d) VT = 15 ml/kg, RR = 20 b/min, (e) VT = 10 ml/kg, RR = 30 b/min, (f) VT = 12 ml/kg, RR = 30 b/min, (g) VT = 10 ml/kg, RR = 35 b/min, (h) VT = 12 ml/kg, RR = 35 b/min, (i) VT = 10 ml/kg, RR = 40 b/min, (j) VT = 12 ml/kg, RR = 40 b/min.